

Plasma Membrane Calcium ATPases Are Important Components of Receptor-Mediated Signaling in Plant Immune Responses and Development^{1[C][W][OA]}

Nicolas Frei dit Frey², Malick Mbengue, Mark Kwaaitaal, Lisette Nitsch, Denise Altenbach, Heidrun Häweker, Rosa Lozano-Duran, Maria Fransiska Njo, Tom Beeckman, Bruno Huettel, Jan Willem Borst, Ralph Panstruga, and Silke Robatzek*

Max-Planck-Institute for Plant Breeding Research, 50829 Cologne, Germany (N.F.d.F., M.K., D.A., H.H., B.H., R.P., S.R.); The Sainsbury Laboratory, Norwich NR4 7UH, United Kingdom (M.M., H.H., R.L.-D., S.R.); Wageningen University, Laboratory of Biochemistry, Microspectroscopy Centre, 6703HA Wageningen, The Netherlands (L.N., J.W.B.); Department of Plant Systems Biology, Flanders Institute for Biotechnology, 9052 Ghent, Belgium (M.F.N., T.B.); Department of Plant Biotechnology and Bioinformatics, Ghent University, 9052 Ghent, Belgium (M.F.N., T.B.); and Rheinisch Westfälische Technische Hochschule Aachen University, Institute for Biology I, Unit of Plant Molecular Cell Biology, 52056 Aachen, Germany (R.P.)

Plasma membrane-resident receptor kinases (RKs) initiate signaling pathways important for plant immunity and development. In *Arabidopsis* (*Arabidopsis thaliana*), the receptor for the elicitor-active peptide epitope of bacterial flagellin, flg22, is encoded by FLAGELLIN SENSING2 (FLS2), which promotes plant immunity. Despite its relevance, the molecular components regulating FLS2-mediated signaling remain largely unknown. We show that plasma membrane ARABIDOPSIS-AUTOINHIBITED Ca²⁺-ATPase (ACA8) forms a complex with FLS2 in planta. ACA8 and its closest homolog ACA10 are required for limiting the growth of virulent bacteria. One of the earliest flg22 responses is the transient increase of cytosolic Ca²⁺ ions, which is crucial for many of the well-described downstream responses (e.g. generation of reactive oxygen species and the transcriptional activation of defense-associated genes). Mutant *aca8 aca10* plants show decreased flg22-induced Ca²⁺ and reactive oxygen species bursts and exhibit altered transcriptional reprogramming. In particular, mitogen-activated protein kinase-dependent flg22-induced gene expression is elevated, whereas calcium-dependent protein kinase-dependent flg22-induced gene expression is reduced. These results demonstrate that the fine regulation of Ca²⁺ fluxes across the plasma membrane is critical for the coordination of the downstream microbe-associated molecular pattern responses and suggest a mechanistic link between the FLS2 receptor complex and signaling kinases via the secondary messenger Ca²⁺. ACA8 also interacts with other RKs such as BRI1 and CLV1 known to regulate plant development, and both *aca8* and *aca10* mutants show morphological phenotypes, suggesting additional roles for ACA8 and ACA10 in developmental processes. Thus, Ca²⁺ ATPases appear to represent general regulatory components of RK-mediated signaling pathways.

Receptor kinases (RKs) constitute a large gene family in plants, with more than 600 members in *Arabidopsis* (*Arabidopsis thaliana*), and are key to ligand-mediated signaling pathways in plant immunity and development (Shiu and Bleecker, 2001). Only a handful of RKs

have been studied in detail and matched with their cognate ligand, of which FLAGELLIN SENSING2 (FLS2), EF-TU RECEPTOR (EFR) from *Arabidopsis*, and rice XA21 encode Leu-rich repeat-RKs, conferring the perception of microbe-associated molecular patterns (MAMPs) from bacteria in these plants (Zipfel, 2009). Perception of the fungal MAMP chitin involves the LysM-RK CHITIN ELICITOR RECEPTOR KINASE1. FLS2 detects a conserved peptide at the N terminus of bacterial flagellin (flg22) and forms an inducible complex with BRI1-ASSOCIATED KINASE1/SOMATIC EMBRYO RECEPTOR KINASE3 (BAK1/SERK3), a Leu-rich repeat-RK initially identified as a coreceptor of BRASSINOSTEROID INSENSITIVE1 (BRI1) regulating brassinosteroid signaling and now reported to also act in various immune pathways and cell death control (Chinchilla et al., 2009; Postel et al., 2010; Schulze et al., 2010; Fradin et al., 2011; Schwessinger et al., 2011). The manifold phenotypes of *bak1/serk3* mutant plants suggest that BAK1/SERK3 can potentially interact with multiple RKs to regulate a number of different signaling pathways. This offers the

¹ This work was supported by the German Research Council (grant no. SFB670) and the Gatsby Charitable Foundation.

² Present address: INRA-CNRS, UMR1165, Unité de Recherche en Génomique Végétale, 2 rue Gaston Crémieux, F-91057 Evry, France.

* Corresponding author; e-mail robatzek@tsl.ac.uk.

The author responsible for distribution of materials integral to the findings presented in this article in accordance with the policy described in the Instructions for Authors (www.plantphysiol.org) is: Silke Robatzek (robatzek@tsl.ac.uk).

^[C] Some figures in this article are displayed in color online but in black and white in the print edition.

^[W] The online version of this article contains Web-only data.

^[OA] Open Access articles can be viewed online without a subscription.

www.plantphysiol.org/cgi/doi/10.1104/pp.111.192575

possibility for molecular cross talk between different RK-mediated signaling pathways, as recently demonstrated for brassinosteroid signaling negatively impacting flg22 responses (Albrecht et al., 2012; Belkadir et al., 2012). At the molecular level, BAK1/SERK3 was shown to transphosphorylate BRI1 and EFR (Wang et al., 2008; Chen et al., 2010; Schwessinger et al., 2011). Moreover, BRI1, FLS2, and EFR can associate with other members of the SERK family, revealing some levels of functional redundancy (Albrecht et al., 2008; Roux et al., 2011).

Interaction between the ligand-binding RKS BRI1, FLS2, EFR, and BAK1/SERK3 is required for proper downstream responses (Chinchilla et al., 2007). Among the earliest responses stimulated by MAMPs are changes in ion fluxes across the plasma membrane, which result in an increased level of calcium ions (Ca^{2+}) in the cytosol (Blume et al., 2000; Wendehenne et al., 2002; Jeworutzki et al., 2010). Ca^{2+} acts as an important second messenger for a multitude of biotic and abiotic stimuli, whereas different signals trigger unique Ca^{2+} signatures (Dodd et al., 2010; Kudla et al., 2010). MAMPs typically induce a transient Ca^{2+} burst, resulting in a rapid (within seconds) increase of free cytosolic Ca^{2+} , which subsequently (within minutes) declines to steady-state Ca^{2+} levels (Blume et al., 2000; Ranf et al., 2008). The Ca^{2+} burst occurs upstream of many MAMP-elicited responses, including the rapid production of reactive oxygen species (ROS), the activation of signaling kinases, as well as changes in gene expression (Blume et al., 2000; Boller and Felix, 2009; Ranf et al., 2011; Segonzac et al., 2011). However, genetic studies and the identification of the underlying molecular components of the MAMP-induced Ca^{2+} burst are largely missing (Ranf et al., 2008; Boller and Felix, 2009). In general, cytosolic Ca^{2+} levels are regulated by plasma membrane- and endomembrane-bound Ca^{2+} channels that mediate the influx of Ca^{2+} and efflux transporters that reestablish Ca^{2+} homeostasis. A number of ion channels have been identified, some of which have roles in plant immunity, such as DEFENSE NO DEATH1 (DND1; Clough et al., 2000; Lamotte et al., 2004; Kudla et al., 2010). Recently, ionotropic Glu receptor-like proteins were shown to regulate Ca^{2+} influx at the plasma membrane and were also implicated in MAMP-induced responses (Cho et al., 2009; Kwaaitaal et al., 2011; Michard et al., 2011; Vatsa et al., 2011), and an endoplasmic reticulum-localized P2A-type Ca^{2+} ATPase was described to contribute to pathogen-induced cell death and to alter the MAMP-triggered Ca^{2+} burst (Zhu et al., 2010). The relevance of the Ca^{2+} influx in MAMP-elicited responses is underlined by polysaccharides secreted from bacterial pathogens to chelate Ca^{2+} in the apoplastic space (Aslam et al., 2008).

Here, we report that the plasma membrane-resident P2B-type Ca^{2+} ATPase ACA8 interacts with FLS2 in planta. Loss-of-function *aca8* plants, the mutant of its closest homolog *aca10*, and the *aca8 aca10* double mutant were more susceptible to bacterial infection. Analyzing individual MAMP responses, *aca8 aca10* mutant plants displayed decreased flg22-triggered Ca^{2+} influx

and ROS accumulation. Importantly, flg22-triggered gene expression downstream of mitogen-activated protein kinase (MAPK) signaling was increased, but gene expression downstream of calcium-dependent protein kinase (CDPK) signaling was reduced. This suggests that the MAMP-induced Ca^{2+} burst is required for proper transcriptional reprogramming upon elicitation. According to their function as Ca^{2+} pumps, ACA8 and ACA10 are hypothesized to regulate Ca^{2+} efflux during the flg22-elicited Ca^{2+} burst, which suggests a molecular link between the FLS2 receptor, Ca^{2+} signaling, and flg22-triggered downstream responses. In addition, *aca10* and *aca8 aca10* mutant plants showed developmental phenotypes affecting inflorescence height as well as root length. Together with the finding that ACA8 also interacts with other RKS such as BRI1 and CLV1, these results suggest that plasma membrane Ca^{2+} ATPases function in multiple RK-mediated signaling pathways.

RESULTS

ACA8 Interacts with FLS2 and Other RKS

In a proteomics approach, we previously isolated proteins colocalizing to FLS2 in plasma membrane microdomains (Keinath et al., 2010). To address whether some of these proteins can associate with FLS2, we focused on Ca^{2+} ATPases, which have also been identified as differentially phosphorylated and transcriptionally induced in response to flg22 (Zipfel et al., 2004; Benschop et al., 2007). ACA8 and ACA10 belong to the family of type 2B autoinhibited Ca^{2+} ATPases consisting of 10 members in Arabidopsis (Supplemental Fig. S1A; Boursiac and Harper, 2007). These Ca^{2+} ATPases comprise 10 transmembrane-spanning domains, harbor a calmodulin-binding domain for autoinhibition of the ATPase active site, and can localize to different membrane compartments (Boursiac and Harper, 2007). ACA8, ACA9, and ACA10 group into a distinct subfamily and accumulate at the plasma membrane (Bonza et al., 2000; Hwang et al., 2000; Lee et al., 2007). Whereas ACA9 expression is restricted to pollen and thereby is critical for pollen tube development, ACA8 and ACA10 are expressed throughout the plant and have not yet been assigned any specific function besides inflorescence growth (Schjøtt et al., 2004).

We transiently expressed FLS2 and ACA8 fused to the N- and C-terminal halves of yellow fluorescent protein (YFP), respectively, in *Nicotiana benthamiana* and examined possible protein-protein interactions by confocal microscopy in a so-called bimolecular fluorescence complementation (BiFC) assay (Bracha-Drori et al., 2004). In this assay, we observed reconstitution of the YFP molecule by the detection of fluorescence when expressing FLS2 fused to both of the YFP halves, indicative of FLS2 homodimerization (Fig. 1A). We also observed BiFC when FLS2 was coexpressed with ACA8. As BiFC assays are based on transient expression in a heterologous system, the tagged proteins can accumulate

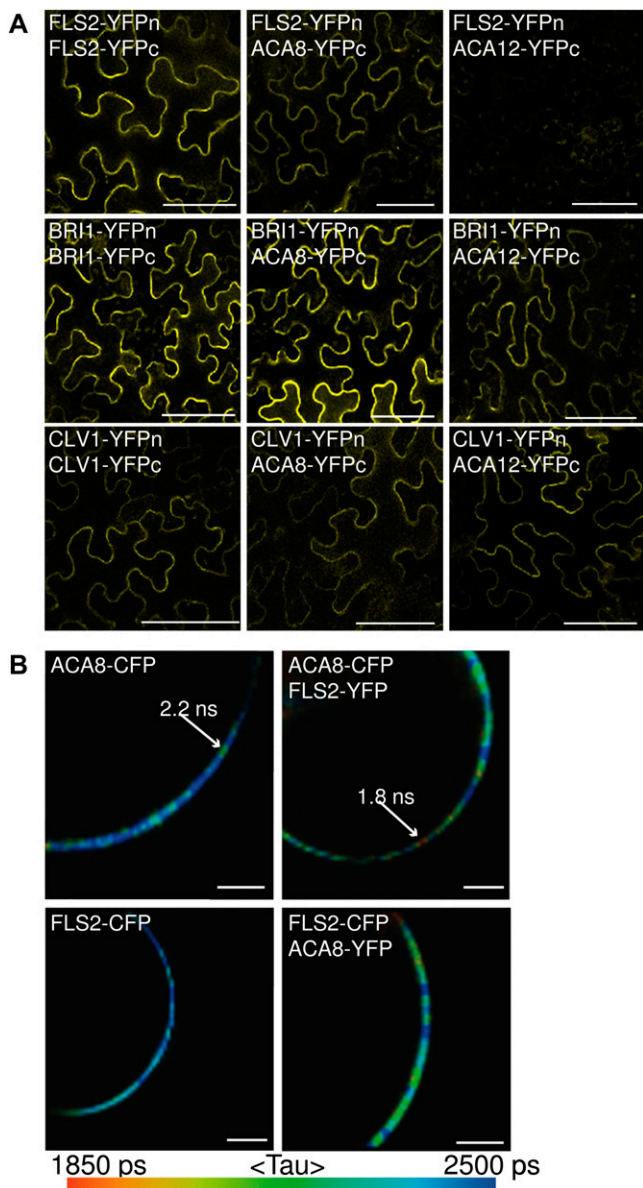


Figure 1. FLS2 interacts with ACA8 in planta. A, BiFC. Representative micrographs show YFP signals of epidermal cells from *N. benthamiana* leaves transformed with plasmids coding for the indicated constructs. YFPc, C-terminal YFP fragment; YFPn, N-terminal YFP fragment. Bars = 100 μm . B, FRET-FLIM measurements. Micrographs show representative false-color-coded fluorescence lifetime images of Arabidopsis protoplasts transfected with plasmids coding for the indicated constructs. Lower fluorescence lifetimes indicate the proximity of the two fluorescence proteins. Similar results were obtained in at least three independent experiments. Bars = 2 μm .

to high levels, facilitating the reconstitution of a BiFC signal; thus, ACA12, BRI1, and CLV1 were included as controls. No YFP reconstitution could be detected upon coexpressing of FLS2 and ACA12, another plasma membrane-resident Ca^{2+} ATPase. Notably, ACA8 showed a broader interaction pattern, because BiFC was also observed with other RKs, such as BRI1 and CLV1, of which the latter is functioning in stem cell

identity maintenance and is normally not expressed in leaf tissue (Waites and Simon, 2000). Similar to FLS2, both BRI1 and CLV1 formed homodimers in this assay, but unlike FLS2, they also interacted with ACA12 (Fig. 1A). In all cases of BiFC, the YFP signal was recorded at the cell periphery, suggesting complex formation at the plasma membrane.

To further overcome the limitations of BiFC assays, we performed Förster resonance energy transfer (FRET) measurements on the basis of fluorescence lifetime imaging microscopy (FLIM) using FLS2 and ACA8 fusions to cyan fluorescent protein (CFP) and YFP, respectively. FRET can be detected using FLIM, where reduction of the fluorescence lifetime of a donor-containing molecule occurs due to the proximity of an acceptor-containing molecule, which is an indication of physical interaction. We examined FLS2-ACA8 association in protoplasts from soil-grown Arabidopsis plants. Under this condition, we observed a significant reduction in fluorescence lifetime when FLS2-CFP and ACA8-YFP were coexpressed as compared with the fluorescence lifetime of ACA8-CFP alone (Fig. 1B; Supplemental Table S1). Similar results were obtained when we used FLS2-CFP and ACA8-YFP. This suggests that both proteins are in close proximity to each other, indicative of a protein-protein interaction. Interaction of fluorophore-tagged FLS2 and ACA8 was detected at the plasma membrane, which is in line with the subcellular localization of the two proteins and substantiates our findings of BiFC in *N. benthamiana*. However, the interaction of fluorophore-tagged FLS2 and ACA8 was not distributed uniformly across the plasma membrane but seen as patchy areas with strongly reduced fluorescence lifetimes (Fig. 1B), which indicates that the presence of FLS2-ACA8 complexes was restricted to subdomains within the plasma membrane. This observation is in agreement with the notion that FLS2 and ACA8 can localize to flg22-induced plasma membrane microdomains (Keinath et al., 2010). Despite numerous attempts, we failed to clone a full-length ACA10 cDNA, which precluded the analysis of ACA10 by fluorophore-based interaction assays. Despite poor results by coimmunoprecipitation analysis, pull-down experiments of FLS2-GFP followed by mass spectrometric analysis repeatedly revealed the presence of ACA8 and ACA10 peptides, further corroborating the existence of FLS2-ACA8 and FLS2-ACA10 complexes in planta (Supplemental Fig. S2). Taken together, these results indicate that FLS2 forms a complex with ACA8 at the plasma membrane and that ACA8 can interact with multiple RKs, pointing at an important role in the regulation of RK-mediated signaling pathways.

ACA8 and ACA10 Exhibit Partial Overlapping Functions

To address ACA8 function, we isolated a T-DNA insertion line and a tilling mutant (both in the ecotype Columbia [Col-0] genetic background) in the ACA8 gene (Supplemental Fig. S1B). Genetic redundancy within members of the ACA family has been documented and

could be expected for members of the *ACA8*, *ACA9*, and *ACA10* subgroup (Boursiac and Harper, 2007). Because *ACA9* expression was specific to pollen tubes, we focused on *ACA10*, isolated a T-DNA insertion line in the *ACA10* gene, and generated *aca8 aca10* double knockout lines (Supplemental Fig. S1C). In addition, we crossed a *35S::ACA8-GFP*-expressing transgenic line into the *aca8 aca10* double mutant. Single *aca8* mutants displayed no obvious developmental phenotypes (Fig. 2). By contrast, *aca10* mutant plants were reduced in inflorescence height and displayed increased axillary stem formation, which was further enhanced in *aca8 aca10* plants (Fig. 2A). This phenotype was also present in *aca10* plants crossed with the *aca8^{Q70*}* tilling mutant (Supplemental Fig. S3) and could be rescued by ectopic *ACA8-GFP* expression, demonstrating functional complementation by the GFP fusion protein (Fig. 2A). Redundant functions of *ACA8* and *ACA10* in the regulation of inflorescence height were previously reported in the Arabidopsis Wassilewskija background (George et al., 2008). Differences between the single mutants may result from an incomplete overlap of the *ACA8* and *ACA10* expression patterns. We did not observe any obvious mutant phenotype in rosette leaf development among the genotypes (Fig. 2B), whereas *aca8 aca10* mutants showed significantly reduced root growth when cultivated in vitro (Fig. 2C). Reduction in root growth was affecting primary root length and could be correlated with an early differentiation of stem cells compared with wild-type plants (Supplemental Fig. S3).

flg22-Triggered Early Responses Depend on *ACA8* and *ACA10* Function

Ca^{2+} ATPases are responsible for extruding Ca^{2+} ions from the cytosol into endomembrane compartments or extracellularly into the apoplast (Bonza et al., 2004; Conn et al., 2011). *ACA8* has been shown to mediate Ca^{2+} transport in yeast and is activated by the binding of calmodulin (CaM) to its N terminus (Bonza et al., 2000, 2004; Mersmann et al., 2010). Based on the interaction of *ACA8* with *FLS2*, we addressed whether *ACA8* and *ACA10* function in the flg22-triggered Ca^{2+} burst. All genotypes, therefore, were crossed to a transgenic line expressing the aequorin (Aeq) Ca^{2+} biosensor (Knight et al., 1991). We performed luminescence-based measurements of free cytosolic Ca^{2+} and revealed slightly elevated constitutive Ca^{2+} levels in *aca8 aca10 Aeq* plants (Supplemental Fig. S4). We then monitored the MAMP-induced Ca^{2+} burst over time. Mutant *aca8 Aeq* and *aca10 Aeq* plants responded like wild-type plants upon flg22 treatment. By contrast, the flg22-triggered Ca^{2+} burst was strongly reduced in the *aca8 aca10 Aeq* lines and completely abolished in *fls2 Aeq* plants (Fig. 3A; Supplemental Fig. S5). The overall pattern of the transient increase of Ca^{2+} remained similar between the wild type and the *aca8 Aeq* and *aca10 Aeq* genotypes, but the maximal influx (peak) of the Ca^{2+} signature was affected in *aca8 aca10 Aeq* plants (Supplemental Fig. S5). The Ca^{2+} burst in response to chitin was slightly reduced in *aca8 aca10 Aeq* lines and

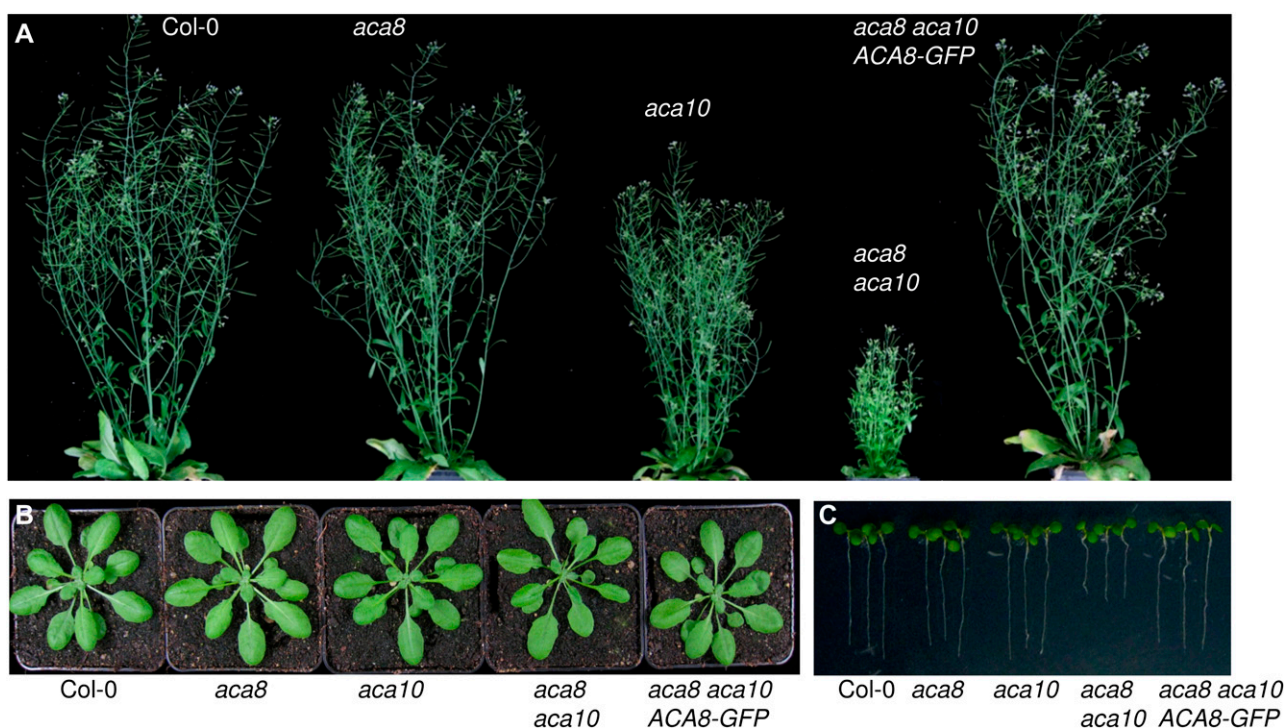


Figure 2. *ACA8* and *ACA10* have a role in plant development. Photographs show growth-related phenotypes of the indicated genotypes in the Col-0 background (Supplemental Fig. S1). A, Inflorescence growth of 8-week-old plants. B, Rosette leaves of 4-week-old plants. C, Root growth of 7-d-old in vitro-grown seedlings.

for all other genotypes was indistinguishable from the wild type (Fig. 3A). The lower peak in flg22-induced cytosolic Ca²⁺ influx in the double mutant demonstrates that ACA8 and ACA10 both contribute to the flg22-elicited Ca²⁺ burst and indicates a role for these proteins in the regulation of FLS2-mediated early responses.

The production of ROS upon MAMP treatments is mediated by plasma membrane-resident NADPH oxidases, which depend on Ca²⁺ signaling for their function (Kobayashi et al., 2007; Mersmann et al., 2010). We examined the flg22-triggered oxidative burst and detected no significant differences between wild-type plants and the *aca8* and *aca10* single mutants, whereas

the *aca8 aca10* double mutant displayed an overall decreased ROS production when treated with flg22 (Fig. 3B). ROS production upon chitin treatment remained comparable to the wild type in all tested mutants. The decrease in oxidative burst correlated with the reduced flg22-triggered Ca²⁺ signature in *aca8 aca10* plants, which is in agreement with Ca²⁺ operating upstream of ROS production. When monitoring these individual MAMP responses, we observed genetic redundancy between *ACA8* and *ACA10*, suggesting that both Ca²⁺ ATPases exert overlapping functions in these early and transient flg22 responses, which is in contrast to the unequal role of *ACA8* and *ACA10* in development. Western-blot analysis revealed unaltered FLS2 protein

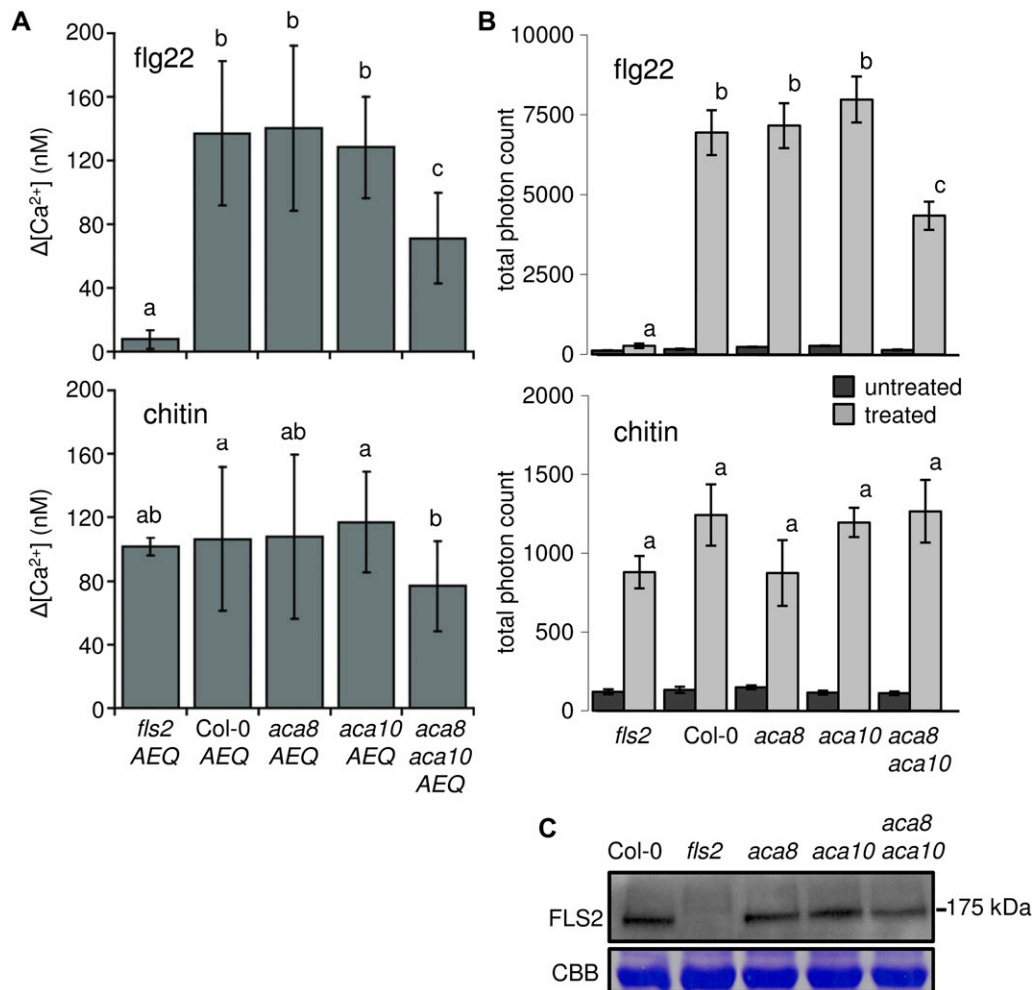


Figure 3. Early MAMP responses are altered in *aca8 aca10* mutants. A, Ca²⁺ burst in response to flg22 and chitin. The *Aeq* Ca²⁺ biosensor was introduced into all indicated genotypes. Data were calculated from curves normalized to steady-state cytosolic [Ca²⁺]. Shown are average changes (Δ) in [Ca²⁺] values in the peak between 4 and 5.5 min after elicitation, which was averaged over two independent biological replicates. Error bars indicate sd based on 14 to 16 samples, and letters indicate significant differences at *P* < 0.05 based on ANOVA with Tukey's honestly significant difference test. B, ROS burst in response to flg22 and chitin. ROS generation (indicated as total photon counts measured between 2 and 30 min upon elicitation) was monitored over time. Error bars indicate sd based on 28 samples, and letters indicate significant differences at *P* < 0.05 based on a *t* test. Similar results were obtained in at least two independent experiments. C, FLS2 protein levels of the indicated genotypes revealed by western blot. Coomassie blue staining (CBB) is included as a loading control. Similar results were obtained in at least two independent experiments. [See online article for color version of this figure.]

accumulation in the *aca* mutants compared with wild-type plants (Fig. 3C). Therefore, the observed reduction in flg22-triggered Ca^{2+} and ROS bursts is likely caused by the loss of *ACA8* and *ACA10* function rather than altered *FLS2* levels.

ACA8 and ACA10 Are Required for Proper flg22-Induced Transcriptional Changes

For more detailed analysis of *ACA8/ACA10* functions, we determined the transcriptional changes caused by *ACA8* and *ACA10* loss of function by microarray analysis. A total of 69 transcripts were identified as showing significantly elevated transcript levels, and 10 had significantly lower transcript abundance in the *aca8 aca10* double mutant compared with wild-type seedlings (Supplemental Table S2 and Supplemental Information S1). We validated the differential transcript accumulation of 19 out of 20 tested genes by quantitative reverse transcription-PCR analysis, of which 17 showed wild-type-like expression in the *aca8 aca10/35S::ACA8-GFP* line, further substantiating the functionality of the *ACA8-GFP* fusion protein (Supplemental Table S2). Most remarkably, genes belonging to the Gene Ontology categories “calcium ion binding” and “cation binding” were overrepresented among the genes that show higher transcript levels in the *aca8 aca10* double mutant (Supplemental Table S2). The first category includes genes coding for CaM-like proteins such as *CML35*, *CML36*, *CML41*, *CML45*, *CML46*, and *CML47* (McCormack et al., 2005). Increased expression of CaM-like genes could be a compensatory mechanism to counteract the deficiency in extruding Ca^{2+} ions from the cytosol in *aca8 aca10* plants.

Only a small number of the *aca8 aca10* deregulated genes were associated with plant defense (Supplemental Table S2). One of them encodes *ACD6*, a regulator of salicylic acid (SA)-mediated disease resistance (Lu et al., 2003). Significantly reduced *ACD6* transcript levels in *aca8 aca10* plants may contribute to the enhanced susceptibility to *Pseudomonas syringae* pv *tomato* DC3000 (*PtoDC3000*). To find out whether any of the other genes that exhibit differential transcript levels in *aca8 aca10* has a potential role in MAMP-triggered immunity, we searched publicly available transcriptome databases and identified 27 of the *aca8 aca10* up-regulated genes to be induced in response to MAMP treatments (Supplemental Fig. S6A). We then focused on genes downstream of flg22 Ca^{2+} signaling (Boudsocq et al., 2010). There was little overlap between the *aca8 aca10* deregulated and CDPK-dependent genes (Supplemental Fig. S6C), which could be due to the different plant materials used for transcript profiling. Therefore, we studied the flg22-induced expression of selected marker genes specifically downstream of the MAPK and/or CDPK cascade (Boudsocq et al., 2010). flg22-induced expression of MAPK-regulated *FLAGELLIN-RESPONSIVE KINASE1* was considerably higher in *aca8 aca10* plants compared with the wild type (Fig. 4). This could point at elevated MAPK signaling in *aca8 aca10*; however, there was no correlation between

flg22-induced MAPK activation and the increased expression of MAPK-specific genes (Supplemental Fig. S7). Induction of the downstream genes cytochrome P450 monooxygenase *CYP81F2*, *FAD-LINKED OXIREDUCTASE*, and *NDR1/HIN-LIKE10*, which are controlled by both the MAPK and CDPK pathways, was either wild type like or somewhat enhanced (Fig. 4). By contrast, the flg22-induced transcript accumulation of the CDPK downstream gene *PHOSPHATE INDUCED1* was notably reduced compared with wild-type levels (Fig. 4). This indicates that gene induction mediated by CDPK signaling is insufficient, likely due to altered flg22 activation of the CDPK cascade.

Our data show that knockout of *ACA8* and *ACA10* function causes pronounced changes in steady-state transcript levels, probably for phenotypic compensation, and also impairs proper flg22-induced transcriptional reprogramming. This was further supported by the differential transcript accumulation of additional marker genes (Supplemental Fig. S8), which either was enhanced (*At5g25250*, *At1g66880*, and *MYB51/At1g18570*) or reduced (*At2g47140* and *WRKY30/At5g24110*) upon flg22 elicitation. We also investigated the flg22-dependent expression of *ACA12* and *ACA13*, which are potential candidates for compensating *ACA8* and *ACA10* loss of function (Supplemental Fig. S1A). After flg22 treatment, both *ACA12* and *ACA13* transcripts accumulated to higher levels in the *aca8 aca10* double mutant background, whereas no significant differences and a slight up-regulation in *ACA12* and *ACA13* abundance, respectively, were detected without MAMP stimulus (Fig. 4). Thus, *ACA12* and *ACA13* may contribute to the control of cytosolic Ca^{2+} levels during flg22 responses. Intriguingly, *ACA12* localizes to the plasma membrane and can interact with the RKs *BRI1* and *CLV1* (Fig. 1A). *ACA12*, however, failed to associate with *FLS2*, which may hamper any possible compensatory effects in flg22 responses.

ACA8 and ACA10 Contribute to Plant Immunity

To examine a possible role of *ACA8* and *ACA10* in plant antibacterial immunity, all genotypes were spray inoculated with virulent *PtoDC3000*, an infection that is defeated utilizing the *FLS2* pathway (Zipfel et al., 2004). Bacterial growth and disease symptom development were monitored 3 and 5 d post inoculation, respectively. *PtoDC3000* multiplied to high titers in *aca8* and *aca10* single mutants as well as in the *aca8 aca10* double mutant, which was comparable to the titers detected in immunocompromised *fls2* mutants (Fig. 5A). This enhanced susceptibility was reduced to wild-type levels in the transgenic *ACA8-GFP* complementation line. Moreover, the disease symptom development of *aca8* and *aca10* single and double mutants was correlated with the enhanced susceptibility phenotype (Fig. 5B). Despite 35S-driven ectopic expression of *ACA8-GFP*, no increased resistance against *PtoDC3000* could be detected in the transgenic line. The *aca8* and *aca10* single mutants were as affected as the *aca8 aca10* double

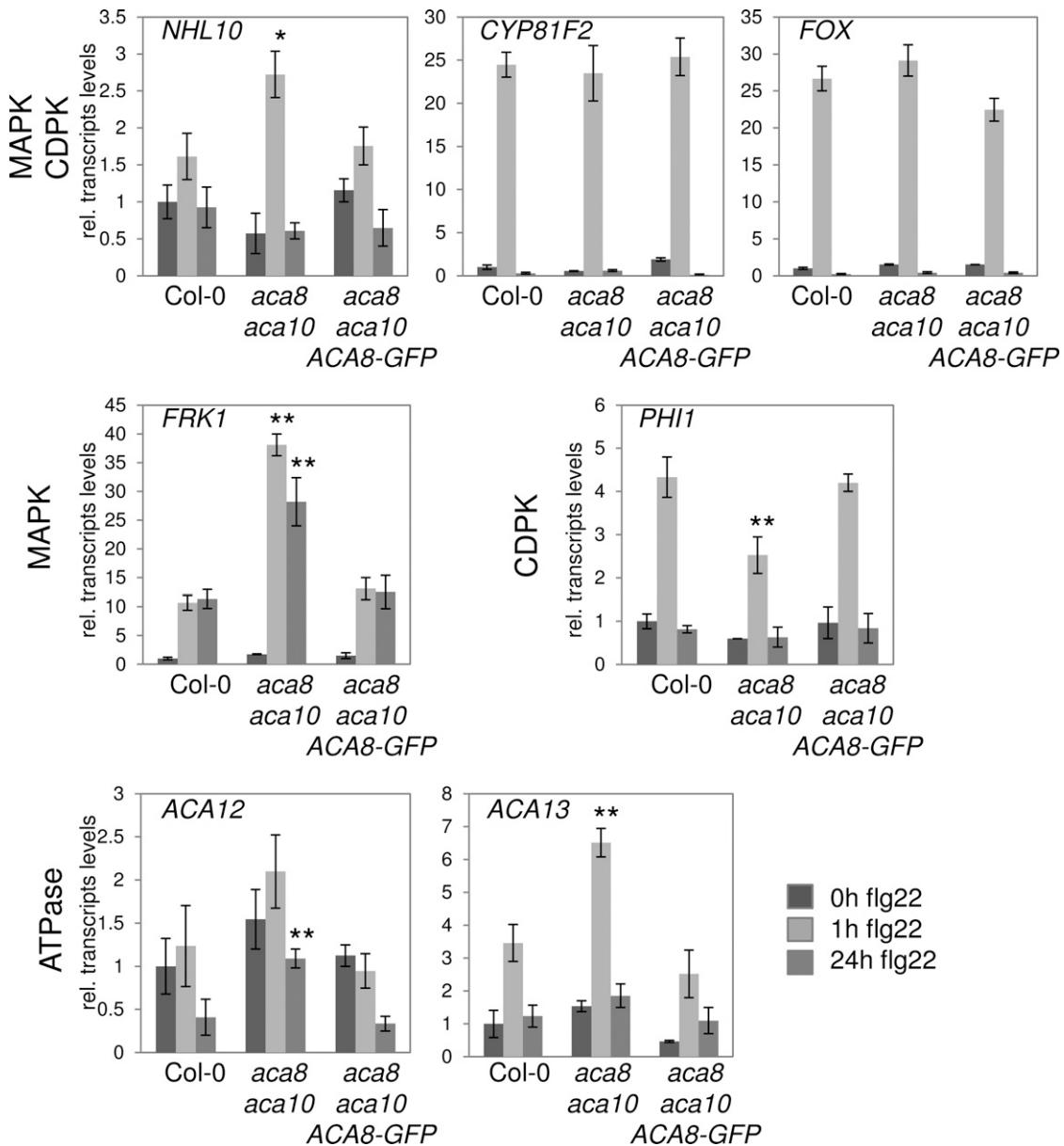


Figure 4. flg22-induced gene expression. Quantitative real-time PCR monitoring is shown for transcript levels of flg22-regulated genes and other Ca²⁺ ATPases in the indicated genotypes upon flg22 elicitation. Actin was used as a control. Error bars indicate SD based on three biological experiments with three technical replicates each; asterisks indicate significant differences between Col-0 and *aca8 aca10* at $P < 0.05$ (*) and $P < 0.01$ (**) based on Student's *t* test. FOX, FAD-LINKED OXIREDUCTASE; FRK1, FLAGELLIN-RESPONSIVE KINASE1; NHL10, NDR1/HIN-LIKE10; PHI1, PHOSPHATE INDUCED1.

mutant upon *Pto*DC3000 infection. Thus, ACA8 and ACA10, both individually and equally, contribute to plant immunity in bacterial infections.

DISCUSSION

It is well known that MAMPs induce a rapid and transient increase of [Ca²⁺] in the cytosol through the function of plasma membrane-resident Ca²⁺ channels (Blume et al., 2000; Ranf et al., 2011), but despite its presumed importance in plant immunity, our current

understanding of how the MAMP-induced Ca²⁺ burst is regulated is rather limited (Ranf et al., 2008; Kudla et al., 2010). Although DND1 is important for cytosolic Ca²⁺ elevation in response to bacterial lipopolysaccharides and endogenous danger peptides (Ma et al., 2009; Qi et al., 2010), it is not required for flg22 and elf18 activation of Ca²⁺ (Jeworutzki et al., 2010). Similarly, the recently suggested Glu receptor-like-type Ca²⁺ channels have been implicated in cryptogei- and flg22-triggered responses by pharmacological approaches; however, genetic evidence for their involvement in MAMP

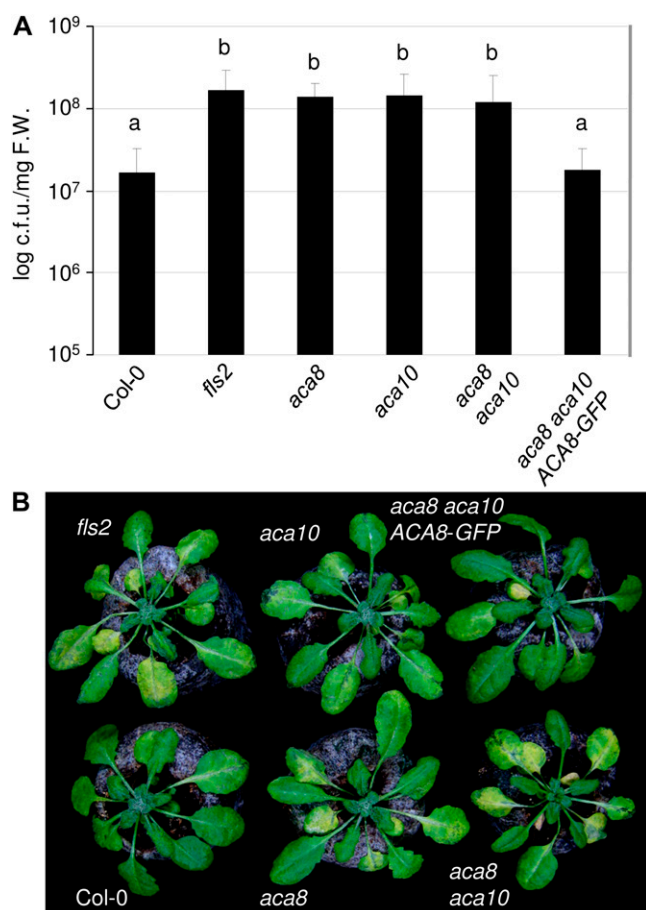


Figure 5. ACA8 and ACA10 contribute to plant immunity. A, Bacterial titers (*PtoDC3000*) in the indicated genotypes (4-week-old plants) at 3 d post inoculation. Error bars indicate SD of three combined independent biological replicates each with six technical replicates; letters indicate significant differences at $P < 0.05$ based on a t test. c.f.u., Colony-forming units; F.W., fresh weight. B, Representative photographs showing macroscopic disease symptoms of 4-week-old plants infected with *PtoDC3000* at 5 d post inoculation.

signaling is still lacking (Kwaaitaal et al., 2011; Michard et al., 2011; Vatsa et al., 2011). Ca^{2+} homeostasis is also controlled through the function of Ca^{2+} ATPases, and our data show that FLS2 forms a complex with ACA8. It is possible that FLS2 transphosphorylates the Ca^{2+} ATPase to regulate its activity, as ACA10 is differentially phosphorylated upon flg22 treatment (Benschop et al., 2007).

Based on our mutant loss-of-function data, ACA8 and ACA10 cofunction to positively regulate the MAMP-induced Ca^{2+} burst. Because of their function as Ca^{2+} pumps, Ca^{2+} ATPases mediate the efflux of Ca^{2+} ions out of the cytosol. Therefore, loss of Ca^{2+} ATPase function should result in an enhanced and prolonged Ca^{2+} burst (Romani et al., 2004). In line with this assumption, Ca^{2+} fluxes triggered by the MAMP cryptogin in *N. benthamiana* were increased in amplitude and duration when endoplasmic reticulum-localized *NbCA1* was silenced (Zhu et al., 2010). Our data on ACA8 and ACA10

unexpectedly revealed a reduction in the MAMP-induced Ca^{2+} burst. We cannot exclude the possibility that other members of the ACA family, such as ACA12 and ACA13, may substitute at least partially for ACA8 and ACA10 function in the mutant backgrounds, as evidenced by the increased ACA12 and ACA13 transcript levels upon flg22 elicitation. This would indicate that the observed phenotypes of *aca8 aca10* mutants are rather an indirect effect. However, ACA12 did not associate with FLS2 in our BiFC analysis, ACA12 and ACA13 transcript levels were not generally increased in *aca8 aca10* mutants, and our transcriptome data did not point at obvious expression changes of any other member of the ACA family. Alternatively, it is possible that the enhanced transcript levels of CaM-like genes in *aca8 aca10* plants reflect a mechanism to compensate for elevated steady-state levels of cytosolic Ca^{2+} . This may in turn lead to the decreased influx of Ca^{2+} into the cytosol, because CaM-like proteins were shown to regulate cyclic nucleotide-gated channels, a class of cation channels with a documented role in Ca^{2+} influx (Ali et al., 2007; Boursiac and Harper, 2007). CaM-like proteins can also activate Ca^{2+} ATPases and are thus key regulators of Ca^{2+} homeostasis (Boursiac and Harper, 2007). However, we cannot exclude a yet unknown modality of Ca^{2+} ATPase function implying a direct rather than indirect action. Based on current knowledge, it is possible to speculate that FLS2 may transiently down-regulate ACA8 and ACA10 activities upon flg22 treatments, thereby allowing a cytosolic Ca^{2+} burst, possibly masked by investigating stable loss-of-function mutants.

The flg22-induced ROS production was decreased in *aca8 aca10* mutants, which is in agreement with a reduction of the flg22-triggered Ca^{2+} burst. Likewise, chemical inhibition of Ca^{2+} ATPase function resulted in reduced ROS production in response to the fungal MAMP oligogalacturonide, placing ACA proteins upstream of RbohD (Romani et al., 2004). As Rboh proteins contain two EF hand motifs in their N-terminal domains (Ogasawara et al., 2008), an altered Ca^{2+} signature in *aca8 aca10* plants may impair ROS generation catalyzed by the NADPH oxidases. In potato (*Solanum tuberosum*), CDPK signaling promotes Rboh-mediated ROS production (Kobayashi et al., 2007). This supports the idea of changed CDPK activation in *aca8 aca10* plants and ACA8/ACA10 regulating kinase signaling, which is substantiated by altered flg22-induced gene expression caused by ACA8 and ACA10 loss of function. The MAPK/CDPK differential gene expression shows that the flg22-induced Ca^{2+} burst is required for the concerted activation of the kinase signaling pathways in order to properly reprogram the transcriptome upon MAMP perception.

Ca^{2+} ATPases have also been shown to regulate defense responses by affecting programmed cell death (Nemchinov et al., 2008). Silencing of *NbCA1* causes an enhanced hypersensitive response cell death upon tobacco mosaic virus activation of the tobacco (*Nicotiana benthamiana*) N immune receptor (Zhu et al., 2010). Knockout plants of ACA4 and ACA11 display cell death-like lesions similar to those triggered by avirulent

pathogens, which were dependent on SA accumulation (Boursiac et al., 2010). Cell death-related phenotypes were not observed in *aca8 aca10* plants. Instead, they were supersusceptible to infection with *PtoDC3000*. Unlike the observed genetic redundancy between ACA8 and ACA10 in plant development and the partial phenotype observed when monitoring individual flg22 responses, the two members of the Ca²⁺ ATPase family are equally required for plant immunity, with single mutants exhibiting a similar level of susceptibility to *fls2* mutants. This apparent difference may be due to the different time frames measuring early flg22 responses and the end point of bacterial infections. A sustained increase of cytosolic Ca²⁺ rather than a transient burst activates downstream defenses (Blume et al., 2000). Additionally, other than MAMP responses, pathogen growth depends on multiple layers of basal immunity (e.g. interference of immunity by effectors from *PtoDC3000*). Effectors can target MAMP receptors at the plasma membrane (Block and Alfano, 2011), or effectors could directly affect the molecular components controlling Ca²⁺ fluxes. Alternatively, perception of the complex mixture of different MAMPs present in *PtoDC3000* may require independent functions of ACA8 and ACA10 or other members of the ACA family. This is supported by the differential expression pattern of *aca8 aca10* deregulated genes in response to flg22 or oligogalacturonides (Supplemental Fig. S6). Moreover, CaM is implicated as a negative regulator in SA-mediated disease resistance, and the CaM-binding protein CBP60g contributes to flg22-elicited SA accumulation and antibacterial defense (Du et al., 2009; Wang et al., 2009), which demonstrates a role for the ACA8/ACA10 deregulated CaM-like genes in plant immunity.

MAMPs are known to trigger a Ca²⁺ burst, one of the most upstream responses in defense signaling (Boller and Felix, 2009; Segonzac et al., 2011). However, the molecular components underlying the complex regulatory network regulating the Ca²⁺ fluxes are still poorly described. In this study, we identified two plasma membrane Ca²⁺ ATPases, ACA8 and ACA10, which, based on mutant loss-of-function data, act as positive regulators of early MAMP responses. Our findings further illustrate the importance of coordinated and fine-tuned MAMP responses, including Ca²⁺ signaling, for plant immunity. Given the altered MAMP-induced MAPK-/CDPK-dependent transcriptional changes together with the ACA8-FLS2 complex formation at the plasma membrane, our results suggest a mechanistic link between the receptor complex and signaling kinases via the secondary messenger Ca²⁺. Although root tip growth upon flg22 treatment and in *fls2* mutants remains to be inspected in more detail, our data also suggest a broader function of Ca²⁺ ATPases in RK-mediated signaling. The functional relevance of the interaction of ACA8 and BRI1 is supported by the *aca8 aca10* mutant phenotype showing defects in the early differentiation of root stem cells (Clouse and Sasse, 1998; Hacham et al., 2011). BRI1-mediated brassinosteroid signaling has been shown to affect root growth through regulation of the cell cycle

(Gonzales-Garcia et al., 2011). Additionally, it is possible that ACA8 and/or ACA10 associate with the Arabidopsis CRINKLY4 RK, known to regulate root stem cells via the CLV3-related peptide CLE40, in particular as root cell type-specific expression data provide evidence for ACA10 transcripts accumulating around the stem cell niche (Brady et al., 2007; Winter et al., 2007; De Smet et al., 2008; Stahl et al., 2009). In analogy to the multiple roles of the coreceptor BAK1/SERK3, this places plasma membrane Ca²⁺ ATPases as important components of RK signaling pathways, likely through the regulation of Ca²⁺ fluxes in the cytosol. Dissecting the precise molecular mechanism of the RK-Ca²⁺ ATPase interaction will further advance our understanding of receptor-mediated signal transduction in the future.

MATERIALS AND METHODS

Plant Lines and Growth Conditions

T-DNA lines for Arabidopsis (*Arabidopsis thaliana*) ACA8 (GK-688H09) and ACA10 (GK-044H01) were obtained from the European Seed Stock Center Nottingham Arabidopsis Stock Centre (<http://arabidopsis.info/>), and the tilling ACA8^{Q70*} line was obtained from the Seattle Tilling Project (<http://tilling.fhcrc.org/>). Homozygous insertions of all *aca8*, *aca10*, *aca8 aca10*, *aca8^{Q70*}*, and *aca8^{Q70*} aca10* mutant plants were validated in the F2 populations by PCR and sequencing. 35S::ACA8-GFP, 35S::Aeq transgenic, and *fls2* mutant lines were described previously (Knight et al., 1991; Zipfel et al., 2004; Lee et al., 2007). Homozygous crossed *aca8 aca10* ACA8-GFP, *aca8 Aeq*, *aca10 Aeq*, *aca8 aca10 Aeq*, and *fls2 Aeq* were confirmed by PCR (all oligonucleotides used in this study are summarized in Supplemental Table S3). Arabidopsis plants grown on soil were kept under short-day conditions for 4 to 5 weeks. Arabidopsis seedlings were grown in vitro on plates or in liquid containing Murashige and Skoog (MS) medium and 1% Suc and kept under long-day conditions for 10 to 14 d. *Nicotiana benthamiana* plants were soil grown under long-day conditions for 4 to 5 weeks.

BiFC

FLS2-Yc, FLS2-Yn, BRI1-Yc, BRI1-Yn, CLV1-Yc, CLV1-Yn, ACA8-Yc, ACA8-Yn, ACA12-Yc, and ACA12-Yn constructs were made by PCR cloning the corresponding full-length cDNAs using Gateway technology in the pAMPAT destination vector series and introduced into *Agrobacterium tumefaciens* strain GV3101 carrying the p19 silencing suppressor (Voinnet et al., 2003; Lefebvre et al., 2010). Overnight cultures were diluted to an optical density at 600 nm of 0.1 in water supplemented with 100 μ M acetosyringone and inoculated into 4-week-old *N. benthamiana* leaves. Leaf samples were imaged at 1 d post inoculation using a Leica confocal TCS SP5 microscope with the Leica LAS AF system software. YFP emission and chlorophyll autofluorescence were detected at emission spectra of 520 to 600 nm and 680 to 780 nm, respectively, after excitation at 488 nm. All samples were imaged with a 20 \times objective. Photographs were taken in line averaging of four scans. The same confocal settings were used to image all samples. Representative images of over three biological replicates are shown.

FRET-FLIM Measurements

FLS2-CFP, FLS2-YFP, ACA8-CFP, and ACA8-YFP constructs were PCR cloned as the corresponding full-length cDNAs using Gateway technology in the pCZN575 and pCZN576 vectors and improved sCFP3A and sYFP2 chromophore variants, respectively (Kremers et al., 2006; Karlova et al., 2011). Constructs were transfected into mesophyll protoplasts from soil-grown Arabidopsis Col-0 plants as described before (Rusina et al., 2004), which were prepared using the tape sandwich method (Wu et al., 2009). FRET-FLIM measurements were performed using the Bio-Rad Radiance 2100 MP system combined with a Nikon TE 300 inverted microscope and a Hamamatsu R3809U MCP PMT (Rusina et al., 2004). FRET between CFP and YFP was detected by monitoring donor emission using a 470- to 500-nm band-pass filter. Images with a frame size of 64 \times 64 pixels were acquired, and the

average count rate was around 0.5×10^4 photons per second for an acquisition time of ± 120 s. Donor fluorescence lifetimes (CFP) were analyzed using SPCImage 3.10 software (Becker & Hickl) using a one- and two-component decay model. Average fluorescence lifetimes of different combinations in several cells ($n > 10$) along the plasma membrane were calculated (Supplemental Table S1). The statistical significance of differences between donor-only and donor-acceptor combinations was determined using Student's *t* test.

Ca²⁺ Measurements

Twelve-day-old sterile-grown seedlings in liquid medium were supplied with 100 μ L of MS medium containing 10 μ M coelenterazine (Biosynth) and dark incubated overnight. Seedlings were supplied with 100 μ L of fresh MS medium and dark incubated for 30 min. Aeq measurements were performed using the Centro LB960 luminometer system (Berthold Technologies). Luminescence from single wells was detected over 0.25 s, and each well was measured every 30 s. After 2 min of measurement, flg22 (EZBiolab) and chitin (Sigma) were added to final concentrations of 1 μ M or 0.1 mg mL⁻¹, respectively, and luminescence was measured over 40 min. For calculation of Ca²⁺ concentrations, 100 μ L of 2 M CaCl₂ in 20% ethanol was added and luminescence was measured over 30 min (0.25 s per well every 63 s). Ca²⁺ concentrations were calculated according to Rentel and Knight (2004). Differences in Aeq levels due to transgene expression and seedling size were corrected by calculating Ca²⁺ concentrations and not using luminescence counts. Per treatment, two assays of eight individual wells were averaged. Ca²⁺ transients were compared between treatments within one experiment unless stated otherwise. Significant differences were evaluated using ANOVA with Tukey's honestly significant difference test.

ROS Measurements

Leaf discs of 5-week-old plants were used for ROS measurements as described previously (Segonzac et al., 2011). Oxidative burst was elicited with 100 nM flg22 or 100 μ g mL⁻¹ chitin oligosaccharide; a negative control without MAMP elicitation was included in all experiments. Luminescence was measured over time using an ICCD photon-counting camera (Photek).

Biochemical Analysis

For western blotting, proteins were separated on 10% SDS-PAGE gels, transferred onto polyvinylidene difluoride membranes using a semidry transfer system, followed by blocking in 5% milk or 3% bovine serum albumin. Antibodies were diluted as follows: anti-p42/44 MAPK (Cell Signaling Technology; 1:1,000), anti-FLS2 (Mersmann et al., 2010; 1:5,000), and alkaline phosphatase-conjugated anti-rabbit (Sigma; 1:20,000–1:30,000). Alkaline phosphatase activity was detected using the CDP-Star (Roche).

For MAPK assay, 14-d-old seedlings grown on MS plates were sprayed with 2 μ M flg22 for 0, 5, 15, or 60 min before harvest. A total of 100 mg of plant material was ground and solubilized in 200 μ L of buffer (50 mM Tris-HCl, pH 7.5, 150 mM NaCl, 10% glycerol, 1 mM EDTA, 10 mM NaF, 2 mM NaVO₃, 25 mM β -glycerophosphate, 1 mM Pefabloc, 1 mM dithiothreitol, 1 mM phenylmethylsulfonyl fluoride, and 0.1% Tween 20) supplied with 3.4 μ L per 100 mg fresh weight protease inhibitor cocktail (Sigma). Extracts were centrifuged, solubilized by 5 min of boiling in 2% SDS Laemmli buffer, and equal amounts were loaded onto SDS gels. MAPK activation was detected with anti-p42/44 MAPK antibodies.

Transcript Profiling

For quantitative reverse transcription-PCR analysis, 14-d-old sterile-grown seedlings were untreated or treated with 1 μ M flg22 for 1 or 24 h. RNA was extracted and DNA digested using the RNeasy Plant Mini Kit and the RNase-Free DNase Set (Qiagen). A total of 2 μ g of RNA was used to synthesize cDNA using the SuperScript II enzyme (Invitrogen). One microliter of a 10 \times dilution of the cDNA was used for each quantitative PCR, using a Bio-Rad iQ5 apparatus and SYBR Green I detection. All oligonucleotides used in this study are summarized in Supplemental Table S3.

Pathogen Infection Assays

Four-week-old soil-grown (Jiffy pellets) Arabidopsis plants were surface inoculated with *Pseudomonas syringae* pv *tomato* DC3000 bacteria at 10⁸ colony-forming units mL⁻¹ and sampled at 3 d post inoculation. Two leaf discs were

pooled from six individual plants, and bacterial extraction was done as described before (Zipfel et al., 2004). The results of three independent experiments were combined, and *t* test analysis was performed.

Sequence data from this article can be found in the GenBank/EMBL data libraries under accession numbers FLS2 (AT5G46330), BRI1 (AT4G39400), CLV1 (AT1G75820), ACA8 (AT5G57110), ACA10 (AT4G29900), and ACA12 (AT3G63380).

Supplemental Data

The following materials are available in the online version of this article.

Supplemental Figure S1. Characterization of ACA8 and ACA10 loss-of-function lines.

Supplemental Figure S2. Identification of ACA8 and ACA10 peptides by mass spectrometry analysis of immunopurified FLS2-GFP.

Supplemental Figure S3. Developmental phenotypes of *aca* mutant plants.

Supplemental Figure S4. Steady-state Ca²⁺ levels before flg22-triggered Ca²⁺ burst and after the burst.

Supplemental Figure S5. Patterns of the Ca²⁺ burst induced by flg22 and chitin over time.

Supplemental Figure S6. Altered gene expression in *aca8 aca10* mutants.

Supplemental Figure S7. Protein kinase activation in flg22 signaling.

Supplemental Figure S8. Expression analysis of defense marker genes.

Supplemental Table S1. Fluorescence lifetime analysis of the FLS2-ACA8 interaction.

Supplemental Table S2. Microarray expression data of *aca8 aca10* deregulated genes.

Supplemental Table S3. List of all oligonucleotides used in this study.

Supplemental Information S1. Supporting information.

ACKNOWLEDGMENTS

We thank W.S. Chung (Gyeongsang National University) for kindly providing the 35S::ACA8-GFP transgenic line mutant, M. Knight Durham University for the 35S::Aeq line, GABI-KAT for T-DNA insertion lines, and the Seattle Tilling Project for the tilling line. We thank A.M.E. Jones (The Sainsbury Laboratory), J. Sklenar (The Sainsbury Laboratory), and S. Laurent (Max-Planck-Institute Cologne) for technical help, M. Beck (The Sainsbury Laboratory) for constructs, U. Goebel (Max-Planck-Institute Cologne) and E. Ver Loren van Themaat (Max-Planck-Institute Cologne) for data analysis of the Affymetrix Tiling 1.0R array, C. Zipfel (The Sainsbury Laboratory) for providing materials and advice, T. Romeis (Free University Berlin) for fruitful discussions, and G. Oldroyd (John Innes Center Norwich) for reading the manuscript.

Received January 9, 2012; accepted April 24, 2012; published April 25, 2012.

LITERATURE CITED

- Albrecht C, Boutrot F, Segonzac C, Schwessinger B, Gimenez-Ibanez S, Chinchilla D, Rathjen JP, de Vries SC, Zipfel C (2012) Brassinosteroids inhibit pathogen-associated molecular pattern-triggered immune signaling independent of the receptor kinase BAK1. *Proc Natl Acad Sci USA* 109: 303–308
- Albrecht C, Russinova E, Kemmerling B, Kwaaitaal M, de Vries SC (2008) Arabidopsis SOMATIC EMBRYOGENESIS RECEPTOR KINASE proteins serve brassinosteroid-dependent and -independent signaling pathways. *Plant Physiol* 148: 611–619
- Ali R, Ma W, Lemtiri-Chlieh F, Tsaltsas D, Leng Q, von Bodman S, Berkowitz GA (2007) Death don't have no mercy and neither does calcium: *Arabidopsis* CYCLIC NUCLEOTIDE GATED CHANNEL2 and innate immunity. *Plant Cell* 19: 1081–1095
- Aslam SN, Newman MA, Erbs G, Morrissey KL, Chinchilla D, Boller T, Jensen TT, De Castro C, Ierano T, Molinaro A, et al (2008) Bacterial polysaccharides suppress induced innate immunity by calcium chelation. *Curr Biol* 18: 1078–1083

- Belkhadir Y, Jaillais Y, Epple P, Balsemão-Pires E, Dangl JL, Chory J (2012) Brassinosteroids modulate the efficiency of plant immune responses to microbe-associated molecular patterns. *Proc Natl Acad Sci USA* **109**: 297–302
- Benschop JJ, Mohammed S, O'Flaherty M, Heck AJ, Slijper M, Menke FL (2007) Quantitative phosphoproteomics of early elicitor signaling in *Arabidopsis*. *Mol Cell Proteomics* **6**: 1198–1214
- Block A, Alfano JR (2011) Plant targets for *Pseudomonas syringae* type III effectors: virulence targets or guarded decoys? *Curr Opin Microbiol* **14**: 39–46
- Blume B, Nürnberger T, Nass N, Scheel D (2000) Receptor-mediated increase in cytoplasmic free calcium required for activation of pathogen defense in parsley. *Plant Cell* **12**: 1425–1440
- Boller T, Felix G (2009) A renaissance of elicitors: perception of microbe-associated molecular patterns and danger signals by pattern-recognition receptors. *Annu Rev Plant Biol* **60**: 379–406
- Bonza MC, Luoni L, De Michelis MI (2004) Functional expression in yeast of an N-deleted form of At-ACA8, a plasma membrane Ca(2+)-ATPase of *Arabidopsis thaliana*, and characterization of a hyperactive mutant. *Planta* **218**: 814–823
- Bonza MC, Morandini P, Luoni L, Geisler M, Palmgren MG, De Michelis MI (2000) At-ACA8 encodes a plasma membrane-localized calcium-ATPase of *Arabidopsis* with a calmodulin-binding domain at the N terminus. *Plant Physiol* **123**: 1495–1506
- Boudsocq M, Willmann MR, McCormack M, Lee H, Shan L, He P, Bush J, Cheng SH, Sheen J (2010) Differential innate immune signalling via Ca(2+) sensor protein kinases. *Nature* **464**: 418–422
- Boursiac Y, Harper JF (2007) The origin and function of calmodulin regulated Ca²⁺ pumps in plants. *J Bioenerg Biomembr* **39**: 409–414
- Boursiac Y, Lee SM, Romanowsky S, Blank R, Sladek C, Chung WS, Harper JF (2010) Disruption of the vacuolar calcium-ATPases in *Arabidopsis* results in the activation of a salicylic acid-dependent programmed cell death pathway. *Plant Physiol* **154**: 1158–1171
- Bracha-Drori K, Shichrur K, Katz A, Oliva M, Angelovici R, Yalovsky S, Ohad N (2004) Detection of protein-protein interactions in plants using bimolecular fluorescence complementation. *Plant J* **40**: 419–427
- Brady SM, Orlando DA, Lee JY, Wang JY, Koch J, Dinneny JR, Mace D, Ohler U, Benfey PN (2007) A high-resolution root spatiotemporal map reveals dominant expression patterns. *Science* **318**: 801–806
- Chen X, Chern M, Canlas PE, Ruan D, Jiang C, Ronald PC (2010) An ATPase promotes autophosphorylation of the pattern recognition receptor XA21 and inhibits XA21-mediated immunity. *Proc Natl Acad Sci USA* **107**: 8029–8034
- Chinchilla D, Shan L, He P, de Vries S, Kemmerling B (2009) One for all: the receptor-associated kinase BAK1. *Trends Plant Sci* **14**: 535–541
- Chinchilla D, Zipfel C, Robatzek S, Kemmerling B, Nürnberger T, Jones JD, Felix G, Boller T (2007) A flagellin-induced complex of the receptor FLS2 and BAK1 initiates plant defence. *Nature* **448**: 497–500
- Cho D, Kim SA, Murata Y, Lee S, Jae SK, Nam HG, Kwak JM (2009) Down-regulated expression of the plant glutamate receptor homolog AtGLR3.1 impairs long-term Ca²⁺-programmed stomatal closure. *Plant J* **58**: 437–449
- Clough SJ, Fengler KA, Yu IC, Lippok B, Smith RK Jr, Bent AF (2000) The *Arabidopsis* dnd1 "defense, no death" gene encodes a mutated cyclic nucleotide-gated ion channel. *Proc Natl Acad Sci USA* **97**: 9323–9328
- Clouse SD, Sasse JM (1998) Brassinosteroids: essential regulators of plant growth and development. *Annu Rev Plant Physiol Plant Mol Biol* **49**: 427–451
- Conn SJ, Gilliam M, Athman A, Schreiber AW, Baumann U, Moller I, Cheng NH, Stancombe MA, Hirschi KD, Webb AA, et al (2011) Cell-specific vacuolar calcium storage mediated by CAX1 regulates apoplastic calcium concentration, gas exchange, and plant productivity in *Arabidopsis*. *Plant Cell* **23**: 240–257
- De Smet I, Vassileva V, De Rybel B, Levesque MP, Grunewald W, Van Damme D, Van Noorden G, Naudts M, Van Isterdael G, De Clercq R, et al (2008) Receptor-like kinase ACR4 restricts formative cell divisions in the *Arabidopsis* root. *Science* **322**: 594–597
- Dodd AN, Kudla J, Sanders D (2010) The language of calcium signaling. *Annu Rev Plant Biol* **61**: 593–620
- Du J, Xie J, Yue L (2009) Intracellular calcium activates TRPM2 and its alternative spliced isoforms. *Proc Natl Acad Sci USA* **106**: 7239–7244
- Fradin EF, Abd-El-Halim A, Masini L, van den Berg GC, Joosten MH, Thomma BP (2011) Interfamily transfer of tomato Ve1 mediates *Verticillium* resistance in *Arabidopsis*. *Plant Physiol* **156**: 2255–2265
- George L, Romanowsky SM, Harper JF, Sharrock RA (2008) The ACA10 Ca²⁺-ATPase regulates adult vegetative development and inflorescence architecture in *Arabidopsis*. *Plant Physiol* **146**: 716–728
- Gonzalez-Garcia MP, Vilarrasa-Blasi J, Zhiponova M, Divol F, Mora-Garcia S, Russinova E, Cano-Delgado AI (2011) Brassinosteroids control meristem size by promoting cell cycle progression in *Arabidopsis* roots. *Development* **138**: 849–859
- Hacham Y, Holland N, Butterfield C, Ubeda-Tomas S, Bennett MJ, Chory J, Savaldi-Goldstein S (2011) Brassinosteroid perception in the epidermis controls root meristem size. *Development* **138**: 839–848
- Hwang I, Harper JF, Liang F, Sze H (2000) Calmodulin activation of an endoplasmic reticulum-located calcium pump involves an interaction with the N-terminal autoinhibitory domain. *Plant Physiol* **122**: 157–168
- Jeworutzki E, Roelfsema MR, Anshütz U, Krol E, Elzenga JT, Felix G, Boller T, Hedrich R, Becker D (2010) Early signaling through the *Arabidopsis* pattern recognition receptors FLS2 and EFR involves Ca-associated opening of plasma membrane anion channels. *Plant J* **62**: 367–378
- Karlova R, Rosin FM, Busscher-Lange J, Parapunova V, Do PT, Fernie AR, Fraser PD, Baxter C, Angenent GC, de Maagd RA (2011) Transcriptome and metabolite profiling show that APETALA2a is a major regulator of tomato fruit ripening. *Plant Cell* **23**: 923–941
- Keinath NF, Kierszniowska S, Lorek J, Bourdais G, Kessler SA, Shimosato-Asano H, Grossniklaus U, Schulze WX, Robatzek S, Panstruga R (2010) PAMP (pathogen-associated molecular pattern)-induced changes in plasma membrane compartmentalization reveal novel components of plant immunity. *J Biol Chem* **285**: 39140–39149
- Knight MR, Campbell AK, Smith SM, Trewavas AJ (1991) Transgenic plant aequorin reports the effects of touch and cold-shock and elicitors on cytoplasmic calcium. *Nature* **352**: 524–526
- Kobayashi M, Ohura I, Kawakita K, Yokota N, Fujiwara M, Shimamoto K, Doke N, Yoshioka H (2007) Calcium-dependent protein kinases regulate the production of reactive oxygen species by potato NADPH oxidase. *Plant Cell* **19**: 1065–1080
- Kremers GJ, Goedhart J, van Munster EB, Gadella TW Jr (2006) Cyan and yellow super fluorescent proteins with improved brightness, protein folding, and FRET Förster radius. *Biochemistry* **45**: 6570–6580
- Kudla J, Batistic O, Hashimoto K (2010) Calcium signals: the lead currency of plant information processing. *Plant Cell* **22**: 541–563
- Kwaaitaal M, Huisman R, Maintz J, Reinstädler A, Panstruga R (2011) Ionotropic glutamate receptor (iGluR)-like channels mediate MAMP-induced calcium influx in *Arabidopsis thaliana*. *Biochem J* **440**: 355–365
- Lamotte O, Gould K, Lecourieux D, Sequeira-Legrand A, Lebrun-Garcia A, Durner J, Pugin A, Wendehenne D (2004) Analysis of nitric oxide signaling functions in tobacco cells challenged by the elicitor cryptogein. *Plant Physiol* **135**: 516–529
- Lee SM, Kim HS, Han HJ, Moon BC, Kim CY, Harper JF, Chung WS (2007) Identification of a calmodulin-regulated autoinhibited Ca²⁺-ATPase (ACA11) that is localized to vacuole membranes in *Arabidopsis*. *FEBS Lett* **581**: 3943–3949
- Lefebvre B, Timmers T, Mbengue M, Moreau S, Hervé C, Tóth K, Bittencourt-Silvestre J, Klaus D, Deslandes L, Godiard L, et al (2010) A remorin protein interacts with symbiotic receptors and regulates bacterial infection. *Proc Natl Acad Sci USA* **107**: 2343–2348
- Lu H, Rate DN, Song JT, Greenberg JT (2003) ACD6, a novel ankyrin protein, is a regulator and an effector of salicylic acid signaling in the *Arabidopsis* defense response. *Plant Cell* **15**: 2408–2420
- Ma W, Smigel A, Verma R, Berkowitz GA (2009) Cyclic nucleotide gated channels and related signaling components in plant innate immunity. *Plant Signal Behav* **4**: 277–282
- McCormack E, Tsai YC, Braam J (2005) Handling calcium signaling: *Arabidopsis* CaMs and CMLs. *Trends Plant Sci* **10**: 383–389
- Mersmann S, Bourdais G, Rietz S, Robatzek S (2010) Ethylene signaling regulates accumulation of the FLS2 receptor and is required for the oxidative burst contributing to plant immunity. *Plant Physiol* **154**: 391–400
- Michard E, Lima PT, Borges F, Silva AC, Portes MT, Carvalho JE, Gilliam M, Liu LH, Obermeyer G, Feijó JA (2011) Glutamate receptor-like genes form Ca²⁺ channels in pollen tubes and are regulated by pistil D-serine. *Science* **332**: 434–437
- Nemchinov LG, Shabala L, Shabala S (2008) Calcium efflux as a component of the hypersensitive response of *Nicotiana benthamiana* to *Pseudomonas syringae*. *Plant Cell Physiol* **49**: 40–46

- Ogasawara Y, Kaya H, Hiraoka G, Yumoto F, Kimura S, Kadota Y, Hishinuma H, Senzaki E, Yamagoe S, Nagata K, et al (2008) Synergistic activation of the Arabidopsis NADPH oxidase AtrbohD by Ca²⁺ and phosphorylation. *J Biol Chem* **283**: 8885–8892
- Postel S, Küfner I, Beuter C, Mazzotta S, Schwedt A, Borlotti A, Halter T, Kemmerling B, Nürnberger T (2010) The multifunctional leucine-rich repeat receptor kinase BAK1 is implicated in Arabidopsis development and immunity. *Eur J Cell Biol* **89**: 169–174
- Qi Z, Verma R, Gehring C, Yamaguchi Y, Zhao Y, Ryan CA, Berkowitz GA (2010) Ca²⁺ signaling by plant Arabidopsis thaliana Pep peptides depends on AtPepR1, a receptor with guanylyl cyclase activity, and cGMP-activated Ca²⁺ channels. *Proc Natl Acad Sci USA* **107**: 21193–21198
- Ranf S, Eschen-Lippold L, Pecher P, Lee J, Scheel D (2011) Interplay between calcium signalling and early signalling elements during defence responses to microbe- or damage-associated molecular patterns. *Plant J* **68**: 100–113
- Ranf S, Wünnenberg P, Lee J, Becker D, Dunkel M, Hedrich R, Scheel D, Dietrich P (2008) Loss of the vacuolar cation channel, AtTPC1, does not impair Ca²⁺ signals induced by abiotic and biotic stresses. *Plant J* **53**: 287–299
- Rentel MC, Knight MR (2004) Oxidative stress-induced calcium signaling in Arabidopsis. *Plant Physiol* **135**: 1471–1479
- Romani G, Bonza MC, Filippini I, Cerana M, Beffagna N, De Michelis MI (2004) Involvement of the plasma membrane Ca²⁺-ATPase in the short-term response of Arabidopsis thaliana cultured cells to oligogalacturonides. *Plant Biol (Stuttg)* **6**: 192–200
- Roux M, Schwessinger B, Albrecht C, Chinchilla D, Jones A, Holton N, Malinovsky FG, Tör M, de Vries S, Zipfel C (2011) The Arabidopsis leucine-rich repeat receptor-like kinases BAK1/SERK3 and BKK1/SERK4 are required for innate immunity to hemibiotrophic and biotrophic pathogens. *Plant Cell* **23**: 2440–2455
- Russinova E, Borst JW, Kwaaitaal M, Caño-Delgado A, Yin Y, Chory J, de Vries SC (2004) Heterodimerization and endocytosis of Arabidopsis brassinosteroid receptors BRI1 and AtSERK3 (BAK1). *Plant Cell* **16**: 3216–3229
- Schiott M, Romanowsky SM, Baekgaard L, Jakobsen MK, Palmgren MG, Harper JF (2004) A plant plasma membrane Ca²⁺ pump is required for normal pollen tube growth and fertilization. *Proc Natl Acad Sci USA* **101**: 9502–9507
- Schulze B, Mentzel T, Jehle AK, Mueller K, Beeler S, Boller T, Felix G, Chinchilla D (2010) Rapid heteromerization and phosphorylation of ligand-activated plant transmembrane receptors and their associated kinase BAK1. *J Biol Chem* **285**: 9444–9451
- Schwessinger B, Roux M, Kadota Y, Ntoukakis V, Sklenar J, Jones A, Zipfel C (2011) Phosphorylation-dependent differential regulation of plant growth, cell death, and innate immunity by the regulatory receptor-like kinase BAK1. *PLoS Genet* **7**: e1002046
- Segonzac C, Feike D, Gimenez-Ibanez S, Hann DR, Zipfel C, Rathjen JP (2011) Hierarchy and roles of pathogen-associated molecular pattern-induced responses in *Nicotiana benthamiana*. *Plant Physiol* **156**: 687–699
- Shiu SH, Bleecker AB (2001) Receptor-like kinases from Arabidopsis form a monophyletic gene family related to animal receptor kinases. *Proc Natl Acad Sci USA* **98**: 10763–10768
- Stahl Y, Wink RH, Ingram GC, Simon R (2009) A signaling module controlling the stem cell niche in Arabidopsis root meristems. *Curr Biol* **19**: 909–914
- Vatsa P, Chiltz A, Bourque S, Wendehenne D, Garcia-Brugger A, Pugin A (2011) Involvement of putative glutamate receptors in plant defence signaling and NO production. *Biochimie* **93**: 2095–2101
- Voinnet O, Rivas S, Mestre P, Baulcombe D (2003) An enhanced transient expression system in plants based on suppression of gene silencing by the p19 protein of tomato bushy stunt virus. *Plant J* **33**: 949–956
- Waites R, Simon R (2000) Signaling cell fate in plant meristems: three clubs on one toulse. *Cell* **103**: 835–838
- Wang L, Tsuda K, Sato M, Cohen JD, Katagiri F, Glazebrook J (2009) Arabidopsis CaM binding protein CBP60g contributes to MAMP-induced SA accumulation and is involved in disease resistance against *Pseudomonas syringae*. *PLoS Pathog* **5**: e1000301
- Wang X, Kota U, He K, Blackburn K, Li J, Goshe MB, Huber SC, Clouse SD (2008) Sequential transphosphorylation of the BRI1/BAK1 receptor kinase complex impacts early events in brassinosteroid signaling. *Dev Cell* **15**: 220–235
- Wendehenne D, Lamotte O, Frachisse JM, Barbier-Brygoo H, Pugin A (2002) Nitrate efflux is an essential component of the cryptogaine signaling pathway leading to defense responses and hypersensitive cell death in tobacco. *Plant Cell* **14**: 1937–1951
- Winter D, Vinegar B, Nahal H, Ammar R, Wilson GV, Provart NJ (2007) An “Electronic Fluorescent Pictograph” browser for exploring and analyzing large-scale biological data sets. *PLoS ONE* **2**: e718
- Wu FH, Shen SC, Lee LY, Lee SH, Chan MT, Lin CS (2009) Tape-Arabidopsis sandwich: a simpler Arabidopsis protoplast isolation method. *Plant Methods* **5**: 16–26
- Zhu X, Caplan J, Mamillapalli P, Czymmek K, Dinesh-Kumar SP (2010) Function of endoplasmic reticulum calcium ATPase in innate immunity-mediated programmed cell death. *EMBO J* **29**: 1007–1018
- Zipfel C (2009) Early molecular events in PAMP-triggered immunity. *Curr Opin Plant Biol* **12**: 414–420
- Zipfel C, Robatzek S, Navarro L, Oakeley EJ, Jones JD, Felix G, Boller T (2004) Bacterial disease resistance in Arabidopsis through flagellin perception. *Nature* **428**: 764–767